Development and Testing of a Novel High-Damping Chlorobutyl Rubber for Structural Viscoelastic Damper Devices

Roshan-Tabari, F.[1][*] ⊙, Toopchi Nezhad, H.[2] ⊙ and Hashemi Motlagh, G.[3] ⊙

[1] Ph.D. Candidate, Department of Civil Engineering, Razi University, Kermanshah, Iran.
[2] Associate Professor, Department of Civil Engineering, Razi University, Kermanshah, Iran.
[3] Assistant Professor, School of Chemical Engineering, College of Engineering, University of Tehran, Iran.

ABSTRACT: The main objective of this study is to modify the blend formulation of a Chlorobutyl rubber compound to improve its damping properties for structural applications. A new rubber composite was created by adding Acrylonitrile Butadiene Rubber (NBR) and Chlorinated Polyethylene (CPE) to Chlorobutyl rubber. The viscoelastic parameters of the cured original CIIR (control sample) and modified CIIR (i.e., CIIR/NBR/CPE) compounds were determined by Dynamic Mechanical Thermal Analysis (DMTA) in tension mode. Subsequently, cyclic shear tests were performed at room temperature and loading frequencies of 0.5, 0.75, 1 and 3 Hz on prototype viscoelastic damper devices fabricated from the rubber blends. The shear force-deformation hysteresis loops of the prototype dampers at shear strains of 0.5, 1.0 and 1.5 revealed that the viscoelastic properties (i.e., shear storage and loss moduli as well as loss factor) of the modified CIIR significantly improved as compared to the original CIIR. The test results demonstrated an increase exceeding 100% and 160% in the shear storage and loss moduli, respectively, of the modified CIIR compared to the reference CIIR.

Keywords: Viscoelastic Damper, High Damping Rubber, Chlorobutyl, Cyclic Shear Tests, Force-Deformation Hysteresis Loops.

1. Introduction

Viscoelastic dampers are supplemental devices used in structural control to mitigate the seismic response of structures, attenuate wind-induced vibrations in tall buildings (Shu et al., 2022), mitigate the seismic pounding of structures (Ramakrishna and Mohan, 2020; Taleshian et al., 2022) and reduce the vibration of floor diaphragms under live loads (Nikravesh and Toopchi-Nezhad, 2022).

Structural seismic control offers an additional opportunity through an integrated design approach. It enables the creation of new structural forms and configurations, such as slender buildings, without compromising their performance (Castaldo and De Iuliis, 2014). Viscoelastic dampers typically employ one or more elastomeric pads made of high-damping rubber with special formulations.

---

[*] Corresponding author E-mail: h.toopchinezhad@razi.ac.ir

During vibrations of the structure, the elastomeric pads are subjected to cyclic shear deformation and owing to their inherently high damping, they dissipate a significant portion of the structural vibration energy. By using viscoelastic supplemental dampers, in addition to effective damping, the stiffness of the structure also increases. Owing to the viscoelastic nature of the elastomer pads within the damper, the effective damping and stiffness of the dampers are generally affected by strain, excitation frequency and ambient temperature (Achenbach and Duarte, 2003; Christopoulos and Filiatrault, 2006; He et al., 2023; Tsai, 1994; Xiang and Xie, 2021).

Numerous types of structural viscoelastic dampers have been explored in existing literature. These include sandwich viscoelastic dampers (Xu et al., 2021), Rotary Rubber Braced Dampers (RRBDs) (Fazli Shahgoli et al., 2021), Viscoelastic Coupling Dampers (VCDs) (Montgomery and Christopoulos, 2015), Visco-Hyperelastic Dampers (VHDs) (Modhej and Zahrai, 2021), and viscoelastic Tuned Mass Dampers (TMDs) (Nikravesh and Toopchi-Nezhad, 2022). Each of these has the potential to improve the dynamic performance of a variety of structures. In most applications, the energy dissipation of viscoelastic material is achieved through shear strain.

However, there are instances where energy dissipation is facilitated by amplified axial strain (Modhej and Zahrai, 2020, 2022). One of the critical factors affecting the performance of a viscoelastic damper is the inherent damping of the elastomer used in the damper, which is attributed to the molecular structure of the base rubber and combination of the constituent components in the rubber compound. The inherent damping of polyethylene, polymathic methacrylate, polypropylene, Styrene-Butadiene Rubber (SBR), Isobutylene-Isoprene Rubber (IIR), and urethane compounds was investigated (Hujare and Sahasrabudhe, 2014). It was found that the effective damping of polyethylene and IIR (commonly known as butyl) compounds was higher than that of other rubbers. The damping property of IIR can be enhanced using miscible polymer oligomers, such as polyisobutylene, as an additional relaxation component (Xia et al., 2018). The effective damping of rubber can be increased using physical methods. For example, innovative pre-compressed viscoelastic dampers made of Chlorobutyl Rubber (CIIR) have been developed (Ghotb and Toopchi-Nezhad, 2019). By pre-compressing the elastomeric pads, the frictional resistance between the chain molecules of the rubber is increased. This results in an increase in effective damping when the damper pads are subjected to shear strain and the rubber molecules slide against each other. The influence of the compressive load on rate-dependent high-damping rubber bearings was also studied (Wei et al., 2019)

Numerous studies have addressed the improvement in the inherent damping of rubber materials used in viscoelastic dampers by modifying their compound formulations. A compound of EPDM and butyl (IIR) rubber materials with the addition of 20 parts of carbon black and 20 parts of paraffinic oil was found to be a suitable option for producing rubber with high inherent damping (Jose et al., 2009).

Application of a type of modified silica fume as an alternative reinforcing filler to improve the damping properties of natural rubber has been investigated (Suntako, 2017). The addition of different kinds and amounts of organic small molecule modifiers (AO1035, AO60 and AO80) to neat Nitrile-Butadiene Rubber (NBR) for improving its energy dissipation capability has been studied (Ge et al., 2022). The addition of CIIR to a compound with Ethylene Propylene Diene Monomer (EPDM) as the base rubber effectively improved the thermal and mechanical properties of the resulting blend, leading to an increase in its inherent damping at room temperature. However, the inherent

damping of the resulting composition was not higher than that of chlorobutyl alone (Jose et al., 2009; Therattil et al., 2008).

Adding aliphatic C5 resin and aromatic C9 resin to the components of CIIR rubber leads to an increase in the effective damping of the rubber (Zhang et al., 2014). Likewise, the use of terpene resin was found to be effective in regulating glass transition and widening the effective damping temperature range of CIIR (Liu et al., 2019).

The multilayer combination of CIIR and PVC in the rubber compound increases its effective damping over a wider temperature range (Zhang et al., 2015). The viscoelastic properties of NBR and CIIR were investigated in the frequency range of 10-10^5 Hz to evaluate the effect of the carbon black ratio on these properties (Capps and Beumel, 1990).

Lu et al. (2014) developed a high damping rubber at ambient temperatures by combining CIIR, NBR and neoprene. In a composite of CIIR and Lead Zirconate Titanate (PZT), the damping properties were improved by transforming the mechanical energy of vibration into electrical energy using PZT. Another material whose application as a viscoelastic damper has been reported in the literature is silicon rubber (Alhasan et al., 2023).

The inherent damping of rubber varies with temperature and reaches a maximum value at the glass transition temperature (T_g), which usually occurs between -20 °C to -100 °C depending on its molecular structure. A rubber material below its glass transition temperature is brittle and the rubber chains are consolidated without any segmental movement.

When the temperature of the rubber part increases and reaches Tg, segmental movement of the chains is initiated and the part starts to become soft. Therefore, at Tg, a relatively large amount of energy is required to initiate chain movements, at such temperatures, the material can absorb a large amount of energy. However, this property significantly decreases at temperatures above 0° C. Therefore, one of the objectives of improving the viscoelastic properties of rubber is to increase its inherent damping at ambient temperature.

As mentioned, CIIR rubber is one of the rubbers with relatively high damping properties. Similar to many other types of rubber, the inherent damping of CIIR decreases significantly at ambient temperatures above 0° C, rendering its use in supplemental viscoelastic dampers unjustifiable. The objective of this study is to enhance the inherent damping of CIIR at ambient temperatures by improving its compound composition. The mechanical and damping properties of the modified rubber at ambient temperatures were assessed via cyclic shear tests at various shear strains and loading frequencies, which are typically expected in many building structures. In the following sections, the modification of rubber compounds by adding new compositional components, testing methods and determination of the viscoelastic properties of both the reference and modified rubber blends are presented.

2. Modified Chlorobutyl Rubber Blend

The base rubber used in the formulations in this study was of the chlorobutyl (CIIR) type. Chlorobutyl rubber, a relatively high-damping rubber, has a wide range of industrial applications. Butyl rubber is a copolymer of isobutylene and small amounts of isoprene, usually 0.8-2.5 mole%, which provides unsaturated bonds for crosslinking by sulfur curing. Chlorobutyl is produced by the halogenation of butyl rubber. Butyl rubber exhibits good resistance to weathering agents and is highly resistant to air and water penetration (Mark et al., 2013). The addition of halogens increased the polymer chain flexibility of butyl and enhanced its compatibility when combined with polar rubbers. Compared to butyl, chlorobutyl exhibits better damping properties and demonstrates better bonding and compatibility with polar rubbers in the

production of multi-rubber compounds (Hanhi et al., 2020).

Several factors affect the dynamic mechanical properties of elastomeric materials, including excitation frequency, temperature, molecular structure of the base polymer and chemical cross-linking systems. Moreover, the physical properties and viscoelastic behavior of these materials are significantly influenced by reinforcing fillers such as different types of carbon black. During cyclic deformations, the stress and strain are out of phase with each other by a certain angle δ, which falls within the range of 0 to π/2 rad. The behavior of a material is described by a complex elastic modulus that comprises both real and imaginary components. The ratio between the imaginary and real components represents the tangent of the phase angle δ and is often referred to as the loss factor or loss tangent (tan δ) (Capps and Beumel, 1990).

The components of chlorobutyl rubber compounds with their designations used in this study are listed in Table 1. The compounds were prepared by mixing all components except the curing agents in a 60

cc, internal mixer with Banbury-type rotors, Misagh Afzar (Tehran, Iran), at 60 rpm and 130 °C for 10 min. After a day of rest at room temperature and prior to molding, the compounds from the internal mixer were mixed with the curing agents, that is, sulfur, CBS and Zinc Dibenzyldithiocarbamate (ZBEC), in a lab-scale two-roll mill (Berstorff, Hannover, Germany) at room temperature for 20 min. The compounds were molded into 2 mm thick sheets in a hot press at 100 bar and 160 °C for 8 min for DMTA analysis.

The mechanical properties of the rubber under dynamic loading were obtained through DMTA tests using a Netzsch-DMA 242 C instrument capable of determining the mechanical properties of the rubber under dynamic loads at different temperatures and frequencies. In the aforementioned test, which was conducted according to the ASTM D5026 standard (ASTM, 2015), the laboratory rubber samples were subjected to cyclic tensile stresses at a frequency of 1 Hz and the temperature was changed from -100 to +100 °C at a heating rate of 3 °C/min.

Table 1. Components of different rubber formulations

Ingredient (phr)	Compound			
	Ref. CIIR	NBR	CIIR-NBR	Mod. CIIR
CIIR	100	0	80	80
NBR	0	100	20	20
CPE	0	0	0	10
N550	30	30	30	30
Sulfur	2	2	2	2
Paraffinic oil	20	20	20	20
Cumarone resin	3.5	3.5	3.5	3.5
ZnO	5	5	5	5
Acid stearic	1	1	1	1
CBS	1.5	1.5	1.5	1.5
ZBEC	1.5	1.5	1.5	1.5

Figure 1 illustrates the changes in the loss factor (tan δ) in the reference CIIR rubber at ambient temperature. As observed, the tan δ curve in CIIR rubber has a peak value of 1.35 at a temperature of -45 °C. The maximum value of the loss factor for this rubber, similar to other rubbers, occurs at its glass transition temperature,

which is usually much below zero degrees. The mechanical properties of polymers undergo significant changes at the glass transition temperature (Landel and Nielsen, 1993). As shown in Figure 1, the tan δ value of the reference CIIR rubber reached 0.4 at 0 °C and decreased significantly at temperatures above 0 °C. A necessary

requirement for effective performance of a viscoelastic damper is the use of rubber with a high loss factor (damping) within the expected temperature range. The main objective of this study was to achieve a rubber compound with high damping properties under an excitation frequency range of 0.5 Hz to 3 Hz (the dominant frequency range of a wide range of building structures) at room temperature.

A glass transition temperature of -45 °C was assigned to CIIR according to the location of the peak in Figure 1. According to this figure, tan δ of CIIR rubber significantly decreases at temperatures

above 0 °C and has negligible values at room temperature. One way to shift the damping temperature range of CIIR to higher temperatures is to blend CIIR with other compatible rubbers or materials. In this study, NBR with a higher glass transition temperature range and therefore, a higher damping temperature range, was selected to extend the damping temperature range of CIIR. NBR and CIIR contain polar groups that are expected to provide good interactions and compatibility. Therefore, their blends are expected to preserve the mechanical properties of their constituents without severe deterioration.
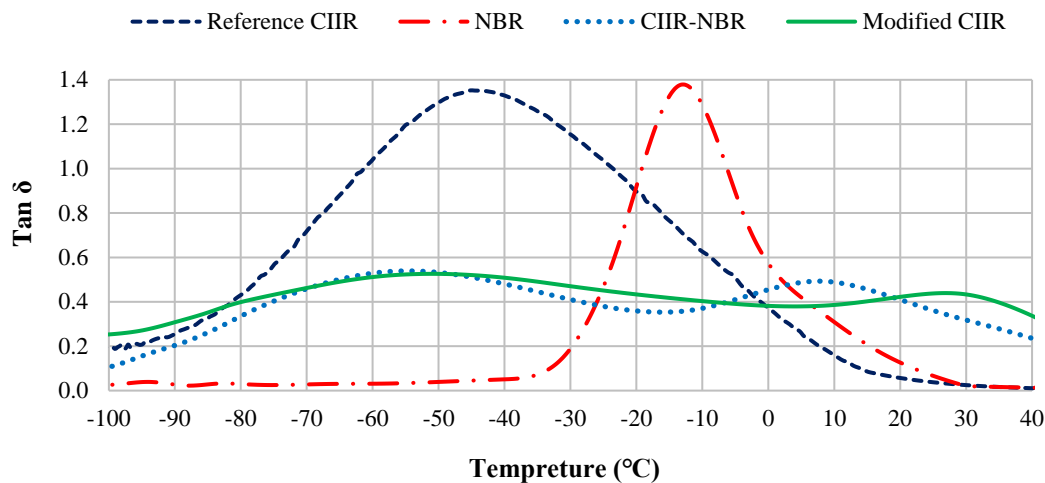
Fig. 1. Variations of the loss factor (tan δ) with temperature for various compounds obtained from DMTA tests conducted at the frequency of 1 Hz

Before blending the two rubbers, it was necessary to determine the changes in the loss factor of NBR with temperature through DMTA tests. The rubber compound formula for NBR (with 33 mole% acrylonitrile) is listed in Table 1 and the variations in the loss factor with temperature (DMTA test results) for this rubber are shown in Figure1. According to Figure 1, the peak loss factor in this rubber is 1.4, which occurs at -17 °C.

Therefore, NBR has an inherent damping capacity that is suitable and comparable to that of CIIR but at higher temperatures. However, the loss factor in the rubber decreased significantly at positive temperatures.

A new compound, CIIR-NBR, was

prepared by blending CIIR with NBR (33 mol% nitrile). The composition of the recently developed compound is presented in Table 1 and the variations in the loss factor with temperature (DMTA test results) for this compound are shown in Figure 1. As observed in Figure 1, by blending these two rubber compounds, the value of tanδ decreased at negative temperatures, but in the positive temperature range, the value of tanδ increased significantly and reached a maximum value of approximately 0.5. In contrast to the previous two compounds, the loss factor curve of CIIR-NBR compound exhibited two peaks at temperatures of -45 ˚C and +22 ˚C. The appearance of these two peaks indicates that the blend was

immiscible. In addition, the corresponding peak of NBR shifted from -17 °C to +22 °C, while that of CIIR remained unchanged.

Therefore, the blend is not sufficiently compatible; otherwise, the temperature peak of CIIR increases and the temperature peak of NBR decreases. The minimum value of the loss factor within the desired temperature range (i.e., ±20 °C) occurs at a temperature close to zero.

At 0 °C, the loss factor decreased by up to approximately 40% compared with its peak value, which was a significant reduction. The significant variations in the loss factor between the two peaks of the CIIR-NBR curve can be attributed to the polar compatibility issues of the blended rubbers.

CIIR rubber has low polarity, whereas NBR has high polarity (Lu et al., 2014). It is noteworthy that the peak temperature of NBR has experienced a significant shift, rising from -17 °C to +22 °C. This enhancement broadens the utility of the blend, particularly as a damper in environments with positive ambient temperatures. As CIIR (1.6 mole% chlorine) and NBR (33 mole% nitrile) are largely different in polarity, this study used CPE as an intermediate material for their compatibility.

In addition, it was of interest to see whether CPE, which is a near-amorphous thermoplastic material with rubbery behavior but a higher glass transition temperature (approximately 0 °C), can increase the damping temperature range of the CIIR/NBR blend.

Hence, the use of CPE extends beyond merely enhancing compatibility between CIIR and NBR. The formula for the newly modified compound, named Modified CIIR, is shown in Table 1. This nomenclature indicates that the base rubber of the modified compound was chlorobutyl rubber. Variations in the loss factor, tanδ, with temperature for the modified chlorobutyl rubber, evaluated using DMTA testing, are shown in Figure 1.

An inspection of this figure shows that the modified composition has a higher loss coefficient than the previous composition (CIIR-NBR) within the temperature range of -40 °C to 15 °C. In the modified chlorobutyl rubber, the minimum tanδ increased from approximately 0.3 to approximately 0.4 with a 33% increase within the temperature range of -40 °C to +25 °C. Additionally, the curve was more uniform in this temperature range, and the maximum variation in tan delta compared to its peak value was approximately -24%.

CPE shifted the corresponding peak of NBR from +22 °C to +30 °C. The damping factor of the modified CIIR was more adequate in the positive temperature range than that of the original CIIR (control sample) up to +35 °C. To investigate the morphology of the compositions at the microscale and compare the fracture surfaces between the phases, SEM images (Figure 2) were used.
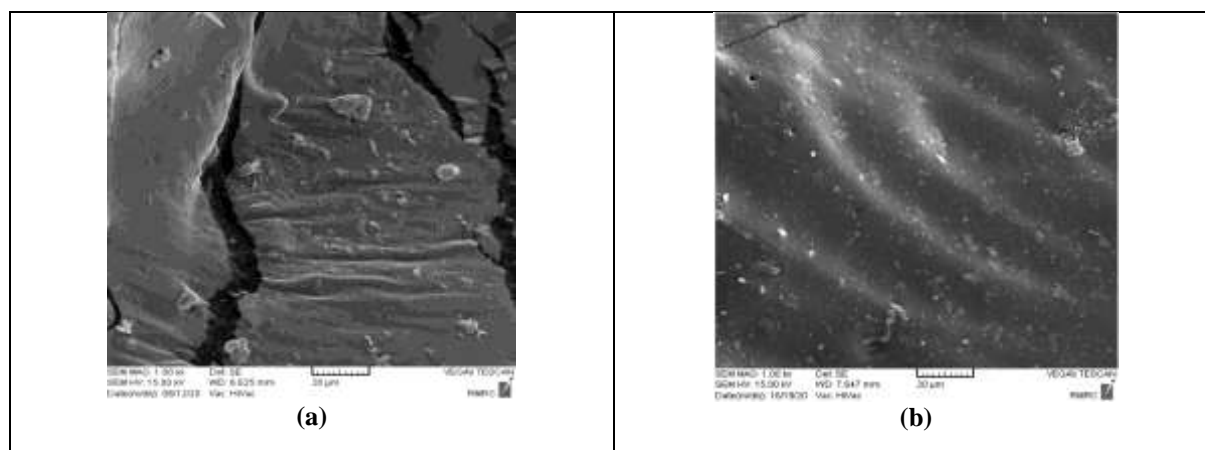
Fig. 2. Microscopic images of rubber compositions before curing: a) CIIR-NBR composition; and b) CIIR-NBR-CPE composition

The microscopic images presented in Figure 2 were captured from the cryo-fractured surfaces of the compounds before curing. A common disperse-matrix morphology for immiscible polymer blends was observed, in which the major polymer (CIIR) was the continuous phase (matrix), and the minor polymer (NBR) was the dispersed phase (particles).

The NBR droplets did not have a spherical shape because of their relative compatibility with the matrix. Figure 2a corresponds to the CIIR-NBR blend. As shown in Figure 2a, the fracture surfaces between the rubber phases were created discontinuously and unevenly with large NBR particles. This defect can cause the formation of small cracks on the macroscopic scale and significantly degrade the properties of the rubber composition. By contrast, Figure 2b corresponds to a rubber composition with 10 CPE parts and it is clear that the fracture surfaces changed from discontinuous and rough to smoother and continuous regions without cracks. More importantly, by adding 10 parts of CPE, the average droplet size of the NBR phase decreased from 8 to 3 µm because of the increased interfacial adhesion between CIIR and NBR provided by CPE as a compatibilizer.

Therefore, it was expected that the final composition would have fewer defects. It appears that CPE serves as a reinforcing agent between two polar and non-polar rubbers, and its elastomeric nature effectively covers the defects between phases. The other CPE dosages were not as effective as 10 phr.

This section pertained to DMTA testing, in which specimens of rubber blends were subjected to dynamic tension. In supplemental viscoelastic dampers, the rubber pads within the damper are typically subjected to cyclic shear deformation. To assess the mechanical response of rubber materials under cyclic shear loads, several prototype viscoelastic dampers have been fabricated using the reference CIIR and Mod. CIIR is the rubber pad of the damper. The test output includes the shear force-deformation hysteresis loops of the prototype dampers under various shear strain amplitudes and excitation frequencies.

2. Prototype Viscoelastic Dampers

To evaluate the viscoelastic hysteretic response of rubber materials under cyclic shear loads, two types of viscoelastic dampers with identical geometrical dimensions but different rubber materials (Ref. CIIR and Mod. CIIR) were fabricated. These damper types are hereafter referred to as Ref. Damper and Mod. Damper, respectively.

Figure 3 shows images of the prototype viscoelastic dampers constructed in this study. As shown in this figure, two individual specimens were fabricated for each type of damper. The geometric dimensions of the dampers were the same for both types, with the only difference being the type of rubber material employed. Figure 4 shows the components of the viscoelastic damper units used in this study.

(a)   (b)

Fig. 3. Damper units of various rubber pads: a) Ref. CIIR pads; and b) Mod. CIIR pads
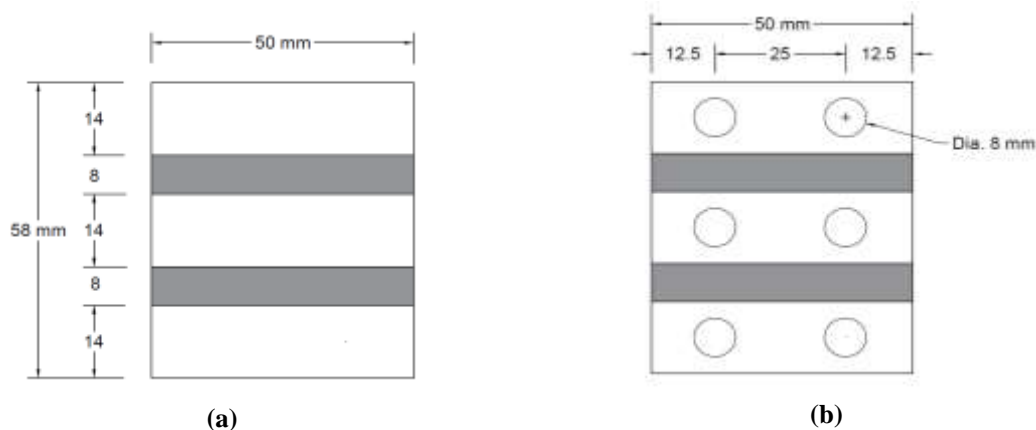
Fig. 4. Sketch of the damper units: a) Front view; and b) Side view

As can be seen in Figures 3 and 4, each unit consisted two layers of rubber pads attached to three metal sheets. The rubber pads were separately vulcanized and bonded to the metal sheets using a cold bonding agent. Threaded holes with diameters of 8 mm were drilled on the opposite sides of the metal sheets to provide support for connecting the inner and outer metal plates of the dampers.

Figure 5 shows the damper assembly and the manner in which the damper unit was attached to the universal fatigue-testing machine. An inner extending Plate (A), was bolted to the inner plate of the damper unit, whereas two outer extending Plates (B), were connected to the outer plates of the damper unit via four bolts (D). To ensure that the damper unit was subjected to pure shear, Plate (C) as an interface plate was inserted between outer Plate B via two E bolts, such that it was perfectly aligned with Plate A. The wedge Grips F of the testing machine were clamped to the roughened ends of Plates A and C. The tensile and compressive forces applied to the specimen via Grips F are transferred to the rubber pads of the damper unit as reciprocating (cyclic) shear forces. Figure 6 shows the images of one of the viscoelastic damper specimens connected to extending Plates A and B, as well as interface Plate C.

Owing to the ability to assemble and disassemble the setup shown in Figures 5 and 6, only one set of Plates A, B and C, was fabricated for all tests conducted in this study. Each of the prototype dampers in this study could be assembled in the aforementioned setup and placed in the fatigue testing machine to perform cyclic shear loading tests.
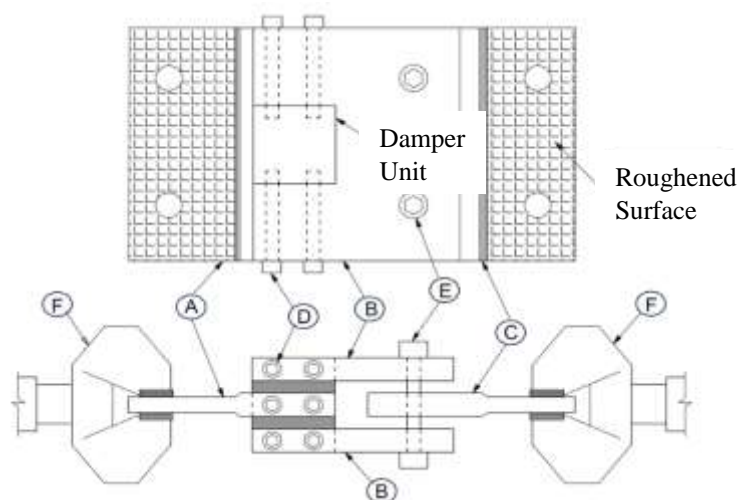
Fig. 5. Components of damper assembly (plan and side views)
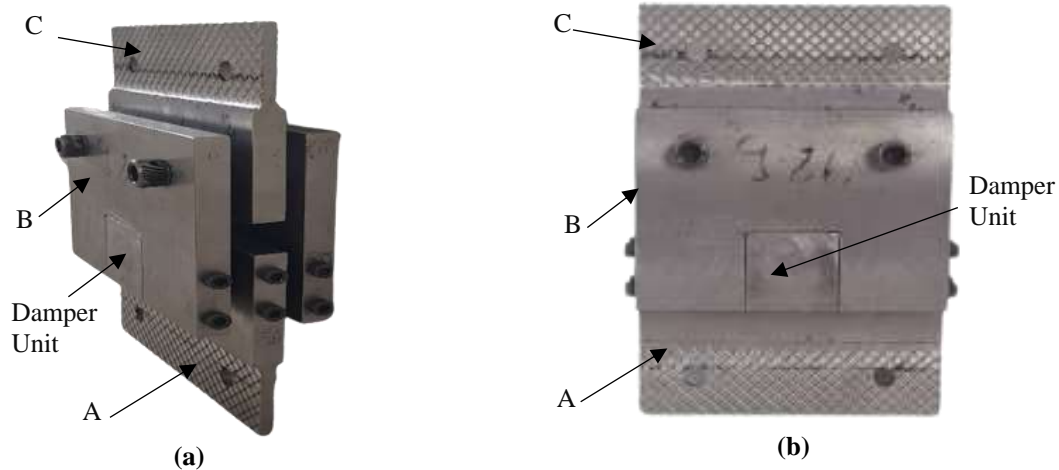
Fig. 6. Assembly of prototype viscoelastic damper: a) 3D view; and b) Front view

Owing to the payload capacity limitations of the test machine, the viscoelastic dampers used in this study were fabricated on a scale of 1:5. It was assumed that by installing supplemental dampers, the performance of the structure would be improved and the story drift ratio would be limited to a maximum of 1% for a Design Basis Earthquake (DBE). Additionally, it was assumed that the damper was installed on rigid chevron bracing; thus, its deformation remained the same as the story drift of the structure. For a typical full-scale story height of 3 m, the displacement amplitude imposed on the damper at the DBE risk level was 30 mm. The corresponding damper displacement was 6 mm, at a scale of 1:5 based on the principles of similitude law (Kahrizi et al., 2022) . If the shear strain of the rubber pads of the damper at this displacement level is limited to 75%, the required thickness of the rubber pads is calculated to be 8 mm. Based on these calculations, the rubber pad thickness within the damper was determined to be 8 mm (Figure 4).

3. Test Protocol and Viscoelastic Response Evaluation

Cyclic shear tests were conducted at ambient temperature to evaluate the shear force-displacement hysteresis loops of the damper specimens and calculate their effective stiffness and damping properties corresponding to various shear strain levels.

Given a target displacement of 8 mm at the DBE, the test protocol included the following stages (ASCE/SEI7, 2017):

i) 10 fully reversed load cycles with a displacement amplitude of 4 mm equivalent to 0.67 times the target displacement at the DBE hazard level.

ii) 5 fully reversed load cycles with a displacement amplitude of 8 mm equivalent to 1.33 times the target displacement at the DBE hazard level.

iii) 3 fully reversed load cycles with a displacement amplitude of 12 mm equivalent to 2 times the target displacement at the DBE hazard level.

Figure 7 shows the time history of sinusoidal input displacements, which is consistent with the loading protocol mentioned above. Input displacements were applied to the prototype dampers with different frequencies in individual test runs.

After the aforementioned cyclic tests were performed, the shear force-displacement curves of the dampers were evaluated. Using the Kelvin solid model, the reaction force in a viscoelastic damper $F(t)$, which is affected by displacement $u(t)$ and velocity $u(t)$, can be obtained from Eq. (1) (Christopoulos and Filiatrault, 2006).

$$F(t) = Ku(t) + Cu(t) \qquad (1)$$

where, K and C: represents the effective stiffness and damping coefficient of the damper specimen, respectively. These parameters can be evaluated at each cycle of

the tests as follows:

$$K = \frac{|F^-| + |F^+|}{|\Delta^-| + |\Delta^+|} \tag{2}$$

$$C = \frac{W_D}{\pi \Delta_{ave}^2 \bar{\omega}} \tag{3}$$

where F^- and F^+: represent the peak negative and positive forces resisted by the damper during the test cycle of negative and positive peak displacement amplitudes Δ^- and Δ^+, respectively. W_D: denotes the area enclosed by the force-displacement hysteresis curve obtained for the load cycle of interest. $\bar{\omega}$: represents the excitation circular frequency, and Δ_{ave} in each load cycle is calculated as below.

$$\Delta_{ave} = \frac{|\Delta^-| + |\Delta^+|}{2} \tag{4}$$

The equivalent viscous damping ratio of the viscoelastic prototype dampers, β, at each cycle of the test can be evaluated as follows.

$$\beta = \frac{1}{2\pi} \frac{W_D}{K \Delta_{ave}^2} \tag{5}$$

The mechanical properties of viscoelastic dampers under cyclic shear loads can be determined at each cycle of the test based on the characteristics of the rubber material within the damper, that is, the storage shear modulus G_e, the shear loss modulus, $G_c\bar{\omega}$, and the loss coefficient η (Smith et al., 1983). In this case, the effect of the physical dimensions of the damper was excluded when comparing the mechanical properties of rubber materials. These parameters can be calculated using the following equations (Christopoulos and Filiatrault, 2006):

$$G_e = \frac{Kh}{A_s} \tag{6}$$

$$G_c = \frac{Ch}{A_s} \tag{7}$$

$$\eta = \frac{G_c\bar{\omega}}{G_e} \tag{8}$$

where h, A_s: are the thickness and plane area of the rubber pad of the damper, respectively. Considering that two rubber pads with the same thickness are used in parallel in the dampers in this study, parameter h is multiplied by 2 in Eqs. (6) and (7). The loss factor η calculated using Eq. (8) represents the tangent of the phase angle δ. The phase angle shows the time delay between the occurrence of the peak shear strain imposed on the rubber material and the peak shear stress experienced therein. The loss factor calculated from Eq. (8) is twice the equivalent critical damping ratio, β, calculated using Eq. (5).
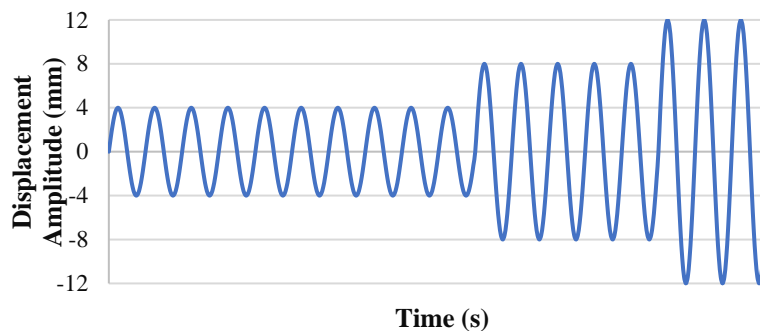
Fig. 7. Time history of input displacements during cyclic shear testing

4. Cyclic Shear Test Results and Discussion

Figure 8 shows the Dartec (UK) fatigue and tensile test machine used for the cyclic loading tests on the prototype viscoelastic dampers used in this study. The machine has a load capacity of 50 kN which can be applied at a maximum loading frequency of 100 Hz, depending on the displacement amplitude of the load cycles.

(a)   **(b)**

Fig. 8. Cyclic shear test setup: a) Installation of damper specimen in test machine; and b) Front view of damper under cyclic loading

(a)   **(b)**
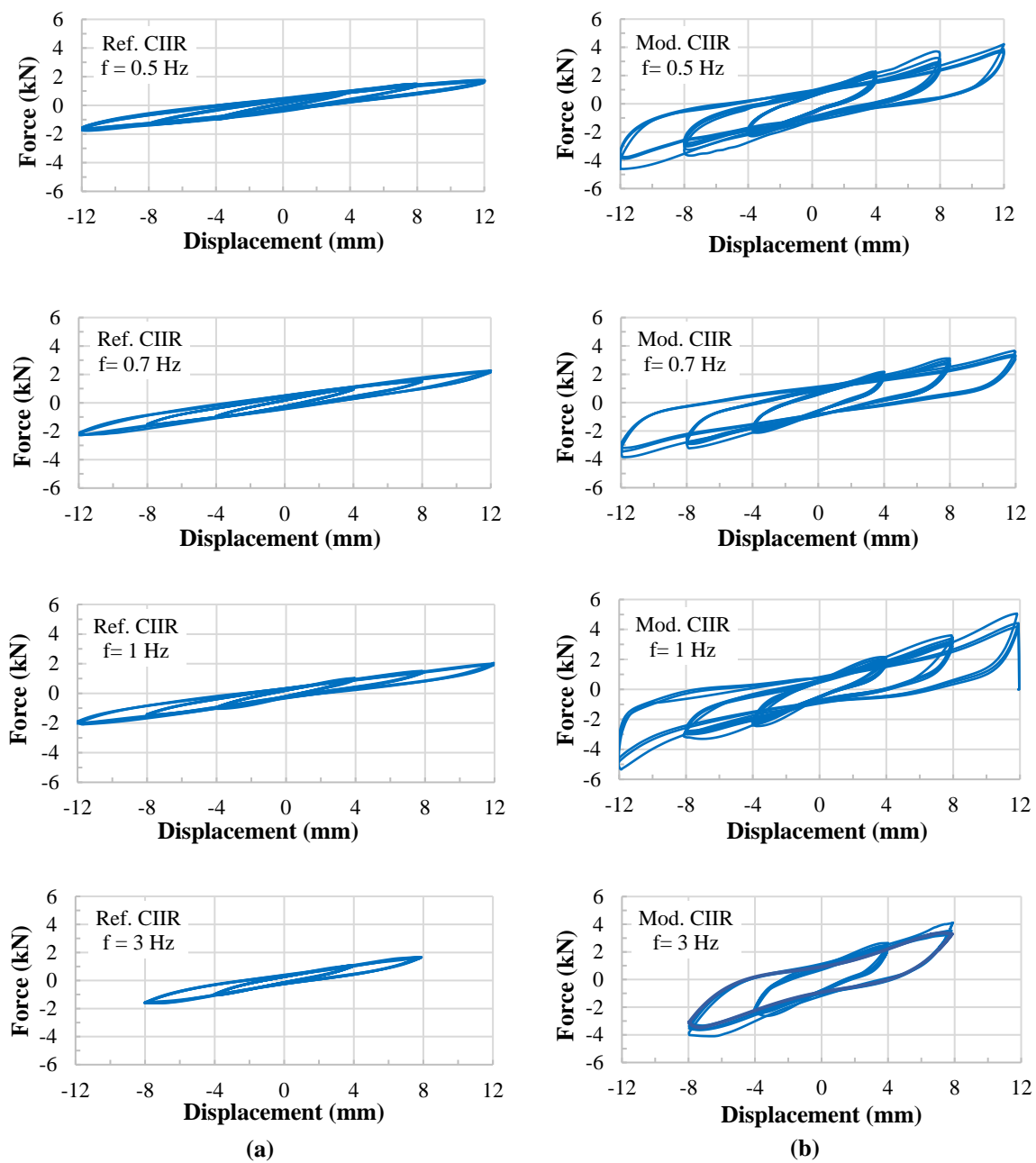
Fig. 9. Cyclic load-displacement hysteresis loops of the damper specimens at various excitation frequencies: a) Reference damper (Ref. CIIR); and b) Modified damper (Mod. CIIR)

It consists of a test frame with a movable crosshead, a piston head with interchangeable load cells and a hydraulic unit that supplies the pressure for the actuator. Given the payload capacity of the test machine, the sinusoidal displacements of the protocol shown in Figure 6 with target displacement amplitudes of 4, 8, and 12 mm, were applied at frequencies of 0.5, 0.7, 1, and 3 Hz.

Moreover, owing to test machine limitations, it was not possible to apply load cycles of different displacement amplitudes in a single test run. Therefore, displacement cycles of the same amplitude were applied individually to the test specimens. The test machine is capable of measuring the axial force and relative displacements of its two jaws in real time. The output of load cell and displacement transducers were recorded by a dynamic data logger at a frequency rate of 50 Hz. All of the tests were performed at room temperature (24 °C).

The force-displacement hysteresis loops of the prototype dampers under fully reversed cycles of shear loading at different excitation frequencies from 0.5 Hz to 3 Hz are shown in Figure 9. At a frequency of 3 Hz, owing to the payload capacity limitation of the testing machine, it was not possible to apply a displacement amplitude of 12 mm and the damper specimens were loaded with this frequency only in the range of 4-8 mm.

Cyclic shear testing of the second specimen of each damper type yielded similar results to those obtained for the first specimen. The variations in the dynamic response parameters (effective stiffness, damping coefficient, and equivalent viscous damping ratio) evaluated for the two specimens of each damper type were less than 10%. This verifies the repeatability of the dynamic response characteristics of each damper type. The damper specimens were visually inspected at the end of each test run to detect physical damage. No significant physical damage was observed in the damper specimens during the testing.

As shown in Figure 9, at all excitation frequencies, the reaction force and area enclosed by the force-displacement hysteresis loops of the modified damper employing Mod. CIIR rubber material was significantly larger than the reference damper. An increase in the reaction force implies an increase in the effective stiffness of the damper in each test cycle. In addition, an increase in the enclosed area of the hysteresis loops indicates the superior energy-dissipation capability of the modified damper.

Figures 10 to 12 show the variations in the shear storage modulus, G_e, shear loss modulus, $G_c\overline{\omega}$, and loss factor, η, of the rubber material of the two damper types with the shear strain amplitude for different excitation frequencies.

Tables 2 and 3 provides the numerical values of the parameters. The viscoelastic parameters shown in these tables and Figures 10-12 represent the average values of the load cycles applied at each displacement amplitude. Parameters G_{e0}, G_{c0} and η_0 in Figures 10-12 represent the average values for the Reference Chlorobutyl Rubber (Ref. CIIR), and likewise G_e, G_c, and η indicate the corresponding values of the Modified Chlorobutyl Rubber (Mod. CIIR). An inspection of Figures 10a and 10b indicates that the shear storage modulus in the modified rubber has a significant increase (at least 100%) compared to the reference rubber.

In both types of rubber materials, at a constant excitation frequency, the shear storage modulus, G_e, decreased with increasing shear strain. This behavior is consistent with the results of previous studies, e.g. Vasina et al. (2021). As shown in Figure 10, the rate of variation of the shear storage modulus with shear strain was similar for both types of rubber materials investigated in this study. By tripling the shear strain (from 0.5 to 1.5), the storage modulus in rubber materials decreases by approximately 30%. According to Figure 10, the shear storage modulus generally increases with increasing excitation frequency.
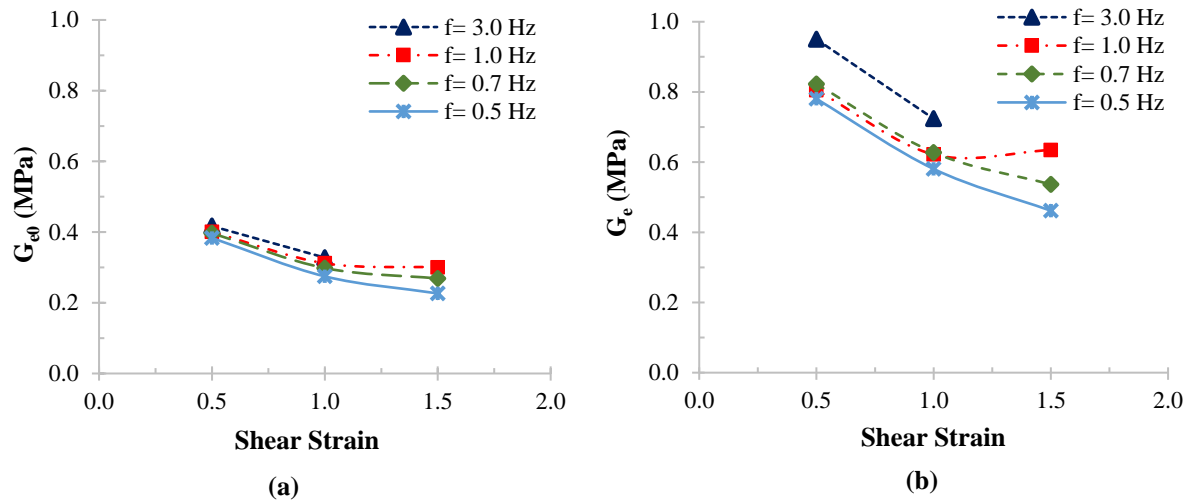
Fig. 10. Variations of shear storage modulus with shear strain at different excitation frequencies: a) Ref. CIIR and b) Mod. CIIR
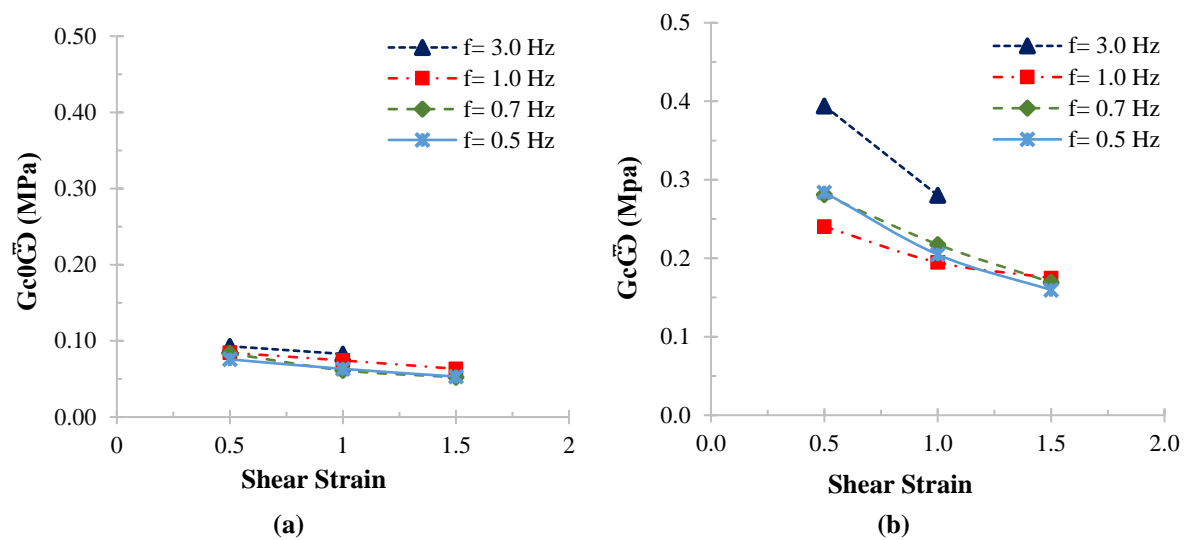
Fig. 11. Variations of shear loss modulus with shear strain at different excitation frequencies: a) Ref. CIIR; and b) Mod. CIIR
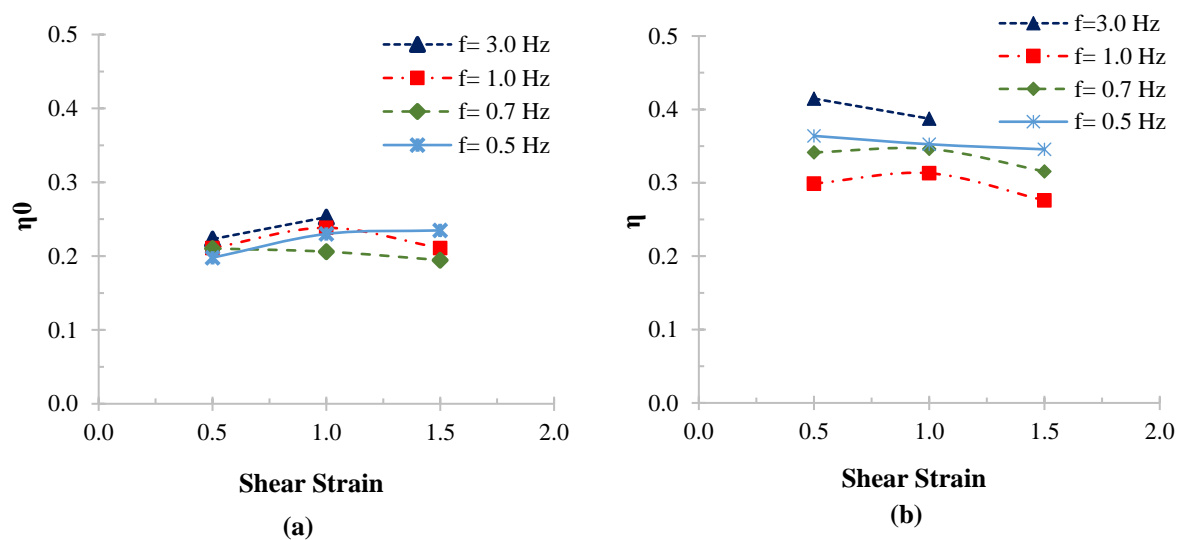
Fig. 12. Variations of loss factor with shear strain at different excitation frequencies: a) Ref. CIIR; and b) Mod. CIIR

Table 2. Viscoelastic properties of reference CIIR

f (Hz)	Amplitude (mm)	G_e (MPa)	$G_c\bar{\omega}$	η
	4	0.38	0.06	0.15
0.5	8	0.27	0.06	0.23
	12	0.23	0.05	0.23
	4	0.40	0.08	0.21
0.7	8	0.31	0.07	0.24
	12	0.30	0.06	0.21
	4	0.40	0.08	0.21
1	8	0.30	0.06	0.21
	12	0.27	0.05	0.19
3	4	0.42	0.09	0.22
	8	0.33	0.08	0.25

Table 3. Viscoelastic properties of modified CIIR

f (Hz)	Amplitude (mm)	G_e (MPa)	$G_c\bar{\omega}$	η
	4	0.82	0.28	0.34
0.5	8	0.63	0.22	0.35
	12	0.54	0.17	0.32
	4	0.78	0.28	0.36
0.7	8	0.58	0.20	0.35
	12	0.46	0.16	0.35
	4	0.80	0.24	0.30
1	8	0.62	0.19	0.31
	12	0.63	0.17	0.28
3	4	0.95	0.39	0.41
	8	0.72	0.28	0.39

The influence of excitation frequency (up to 1 Hz) on the storage modulus of the studied rubber materials at strains of 0.5 and 1 is not significant. At a shear strain of 1.5, the influence of excitation frequency on the shear storage modulus was more noticeable.

In this strain range, the shear storage modulus increased by 32% in the reference rubber and by 37% in the modified rubber with an increase in the excitation frequency from 0.5 Hz to 1 Hz. At the loading frequency of 3 Hz, the shear storage modulus of the modified rubber increased significantly.

At a strain of 0.5, the shear storage modulus of this rubber increased by about 16% from 0.82 MPa at an excitation frequency of 1 Hz to 0.95 MPa at an excitation frequency of 3 Hz. The variation in the shear storage modulus of the reference rubber at an excitation frequency of 3 Hz was not significant compared to other previous lower frequencies. Figure 11 shows the variations in the shear loss modulus with the shear strain applied to rubber materials at different excitation frequencies.

Comparing Figures 11a and 11b, it can be seen that, overall, the shear loss modulus of the modified rubber was approximately three times that of the reference rubber. This revealed that the modifications made to the compound of the reference rubber effectively resulted in a significant increase in the energy dissipation capability of the rubber material. For both rubber types, the shear loss modulus decreased with increasing shear strain. Compared to the reference rubber, the shear loss modulus of the modified rubber was found to be relatively more sensitive to the excitation frequency. A significant increase (approximately 40%) in the shear loss modulus of the modified rubber was observed at an excitation frequency of 3 Hz.

The variations in the loss factor, η, of the rubber materials with the amplitude of shear strain at different excitation frequencies are shown in Figure 11. The loss factor represents the tangent of the phase angle (time lag) between the peak shear stress and the shear strain in the

rubber material at each load cycle. The loss factor values for each test cycle were calculated using Eq. (8). Given the definition of η in Eq. (8) and the decreasing trend of G_e and $G_c\overline{\omega}$ with increasing shear strain for the strain range of 0.5 to 1.5, the loss factor exhibited insignificant variations with shear strain.

Overall, the loss factor in the examined rubber materials at different excitation frequencies varied by $\pm 15\%$ compared with the excitation frequency of 0.5 Hz. At an excitation frequency of 3 Hz, the modified rubber exhibited the highest loss factor. The effective stiffness, K, of the devices can be deduced from Eq. (6). Experimental results demonstrated a substantial enhancement in the stiffness of the modified damper compared to the reference damper. For instance, at the minimal test excitation frequency of 0.5 Hz, the effective stiffness of the reference damper was estimated to range from 0.24 kN/mm (at a displacement amplitude of 4 mm) to 0.14 kN/mm (at a displacement amplitude of 12 mm). In contrast, the modified damper exhibited stiffness values of 0.57 kN/mm and 0.37 kN/mm, respectively, representing an increase of 138% to 164%. Similar enhancements in stiffness properties were observed for the modified damper under cyclic tests with varying excitation frequencies. At the maximal test frequency of 3.0 Hz, the average effective stiffness of the reference damper was calculated to be 0.23 kN/mm, while the modified damper demonstrated an average stiffness of 0.59 kN/mm, marking an approximate increase of 157%. Eq. (7) may be solved for the damping coefficient, C, of the devices. The average damping coefficient for both the reference and modified dampers, at the lowest test excitation frequency of 0.5 Hz, was found to be 0.011 kN.s/mm and 0.051 kN.s/mm, respectively. However, at the highest test frequency of 3.0 Hz, the average damping ratio for the reference damper was determined to be 0.003 kN.s/mm. In contrast, the modified damper exhibited an average damping ratio of 0.013

kN.s/mm, indicating an approximate increase of 333%.

As shown in Figures 10-12, the viscoelastic properties of the modified rubber were significantly higher than those of the reference rubber. Figure 13 shows the ratio of the viscoelastic parameters of the modified rubber to those of the reference rubber at various excitation frequencies under different shear strains.

According to this figure, the ratios of G_e/G_{e0}, G_c/G_{c0}, and η/η_0 depending on the excitation frequency and shear strain amplitude experienced by the rubber material were between 2 to 2.3, 2.6 to 4.3, and 1.3 to 1.9, respectively. An examination of Figure 13 indicates that the ratio of the shear storage moduli of the rubber materials (G_e/G_{e0}) showed the least sensitivity to the excitation frequency and shear strain amplitude.

The ratio of shear loss moduli (G_c/G_{c0}) and loss factors (η/η_0) of the rubber materials did not follow a specific variation with excitation frequency. However, these ratios decreased with an increase in shear strain amplitude.

5. Summary and Conclusions

The main objective of this study was to modify the formulation of a CIIR compound to improve its damping properties under low excitation frequencies at room temperature. The modified rubber was designed as supplemental viscoelastic damper devices to mitigate the earthquake response of building structures. Therefore, by modifying the formulation of the original rubber compound (also referred to as CIIR), a new compound called modified CIIR was prepared, in which NBR and CPE were blended with the reference chlorobutyl rubber in a new formula.

Two sets of tests were conducted to evaluate the viscoelastic characteristics of the rubber. First, the DMTA tests under dynamic tension were performed at a frequency of 1 Hz. Next, cyclic shear tests were conducted on individual prototype

viscoelastic dampers made of the reference and modified rubber materials. Cyclic shear tests were performed at shear strain amplitudes of 0.5, 1.0 and 1.5, under excitation frequencies of 0.5, 0.75, 1.0, and 3 Hz.
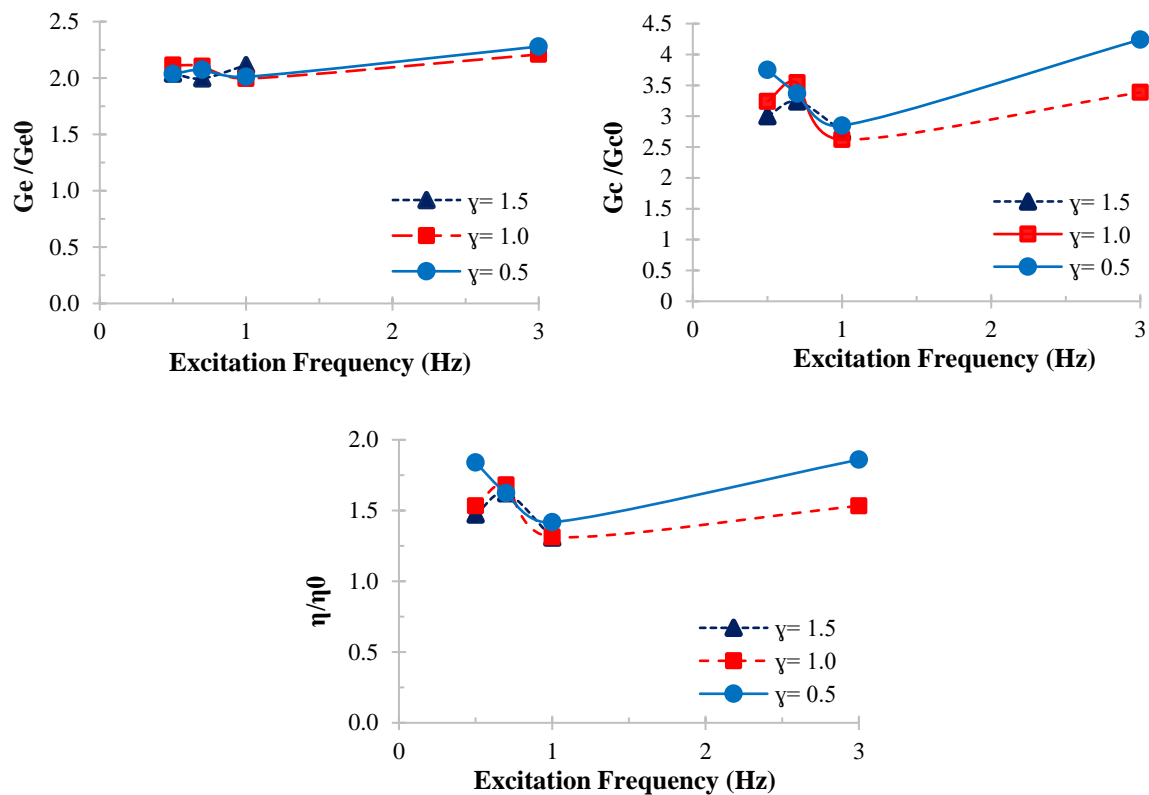
Fig. 13. Variations of the ratio of viscoelastic properties of the modified rubber to the reference rubber with the excitation frequency and shear strain amplitude

The main results obtained from the DMTA tests include:
- In a blend of CIIR and NBR, the magnitude of the loss factor (tanδ), which indicates damping, increased significantly in the positive temperature range and reached a maximum value of approximately 0.5. The variations in tanδ with temperature indicated two peak values at -45 °C and +25 °C. The minimum value of tanδ that occurred at a temperature close to 0 °C was approximately 40% lower than its absolute peak value. The significant variations in tanδ between the two peak values indicated the incompatible polarity of the blended rubber.
- With the use of CPE as an intermediate material in the modified rubber compound, a more polar compatibility was achieved between CIIR and NBR. The two peak values of tanδ occurred at larger temperature intervals (from -50 °C to 30 °C). The modified rubber exhibited a more uniform tanδ over this temperature interval, with a maximum variation of -20% compared to its absolute peak value of 0.5.

The main results obtained from the cyclic shear tests with strain amplitudes ranging from 0.5 to 1.5 and excitation frequencies ranging from 0.5 to 3.0 Hz are as follows:
- The shear storage modulus of the modified CIIR increased on average between 100% and 130% compared to that of the reference CIIR.
- The average shear loss modulus of the modified CIIR increased between 160% and 330% compared to that of the reference CIIR.
- The loss factor, η, of the modified CIIR on average ranged between 0.3 and 0.4, that is, an increase of approximately 30% to 90% compared to the values obtained for the reference CIIR.

- Overall, the viscoelastic parameters of both rubber types exhibited a similar trend of variation with excitation frequency and shear strain amplitude.

The results of this experimental study suggest that the modified CIIR with improved stiffness and damping properties can be effectively used in the fabrication of supplemental viscoelastic damper devices for seismic mitigation of building structures.

6. Data Availability Statement

The experimental data that supports the findings of this study is available from the corresponding author upon reasonable request.

7. Acknowledgements

8. References

Achenbach, M. and Duarte, J. (2003). "A finite element methodology to predict age-related mechanical properties and performance changes in rubber components", *Constitutive Models for Rubber*, (pp. 59-70).

Alhasan, A.A., Vafaei, M. and Ali, S.C. (2023). "Use of silicon rubber as a viscoelastic material in dampers", *IOP Conference Series, Earth and Environmental Science*, https://doi.org/10.1088/1755-1315/1205/1/012047.

ASCE/SEI7. (2017). *Seismic evaluation and retrofit of existing buildings*, ASCE Standard, ASCE/SEI, 41-17, American Society of Civil Engineers, Reston, Virginia, https://doi.org/10.1061/9780784414859.

ASTM. (2015). *Standard test method for plastics, Dynamic mechanical properties, in tension*, In ASTM D5026, American Society for Testing and Materials, PA, United States, https://doi.org/10.1520/D5026-15.

Capps, R.N. and Beumel, L.L. (1990). *Dynamic mechanical testing*, Application of polymer development to constrained-layer damping, ACS Publications, https://doi.org/10.1021/bk-1990-0424.ch004.

Castaldo, P. and De Iuliis, M. (2014). "Optimal integrated seismic design of structural and viscoelastic bracing-damper systems", *Earthquake Engineering and Structural Dynamics*, 43(12), 1809-1827, https://doi.org/10.1002/eqe.2425.

Christopoulos, C. and Filiatrault, A. (2006). *Principles of passive supplemental damping and seismic*, IUSS Press, Pavia, Italy.

Fazli Shahgoli, A., Zandi, Y., Rava, A., Baharom, S., Paknahad, M., Ahmadi, M. and Wakil, K. (2021). "Estimation of the most influential parameters affecting the rotary braces damper", *Iranian Journal of Science and Technology, Transactions of Civil Engineering*, 45, 2463-2475, https://doi.org/10.1007/s40996-02000551-1.

Ge, T., Xu, Z.D. and Yuan, F.G. (2022). "Development of viscoelastic damper based on NBR and organic small-molecule composites", *Journal of Materials in Civil Engineering*, 34(8), 04022192, https://doi.org/10.1061/(ASCE)MT.1943-5533.0004339.

Ghotb, M. and Toopchi-Nezhad, H. (2019). "A feasibility study on pre-compressed partially bonded viscoelastic dampers", *Engineering Structures*, 201, 109796, https://doi.org/10.1016/j.engstruct.2019.109796.

Hanhi, K., Poikelispaa, M. and Tirila, H. (2020). *Elastomeric materials*, Tampere University of Technology, Tampere.

He, Z., Shi, F., Lin, Z., Zhang, C., Zhou, Y. and Zhao, F. (2023). "Experimental characterization on cyclic stability behavior of a high-damping viscoelastic damper", *Construction and Building Materials*, 371, 130749, https://doi.org/10.1016/j.conbuildmat.2023.130749.

Hujare, P.P. and Sahasrabudhe, A.D. (2014). "Experimental investigation of damping performance of viscoelastic material using constrained layer damping treatment", *Procedia Materials Science*, 5, 726733, https://doi.org/10.1016/j.mspro.2014.07.321.

Jose, S.T., Anand, A.K. and Joseph, R. (2009). "EPDM/CIIR blends, improved mechanical properties through procuring", *Polymer Bulletin*, 63, 135-146, https://doi.org/10.1007/s00289-009-0073-8.

Kahrizi, E., Aghayari, R., Bahrami, M. and Toopchi-nezhad, H. (2022). "On compressive stress-strain behavior of standard half-scale concrete masonry prisms", *Civil Engineering Infrastructures Journal*, 55(2), 293-307, https://doi:10.22059/CEIJ.2022.324782.1758.

Landel, R.F. and Nielsen, L.E. (1993). *Mechanical properties of polymers and composites*, CRC Press.

Liu, C., Fan, J. and Chen, Y. (2019). "Design of regulable chlorobutyl rubber damping materials with high-damping value for a wide temperature range", *Polymer Testing*, 79, 106003, https://doi.org/10.1016/j.polymertesting.2019.106003.

Liu, Z., Wang, Y., Huang, G. and Wu, J. (2008). "Damping characteristics of chlorobutyl rubber/poly (ethyl acrylate)/piezoelectric ceramic/carbon black composites", *Journal of Applied Polymer Science*, 108(6), 3670-3676, https://doi.org/10.1002/app.27141.

Lu, X., Li, X. and Tian, M. (2014). "Preparation of high damping elastomer with broad temperature and frequency ranges based on ternary rubber blends", *Polymers for Advanced Technologies*, 25(1), 21-28, https://doi.org/10.1002/pat.3199.

Mark, J.E., Erman, B. and Roland, M. (2013). *The science and technology of rubber*, Academic Press.

Modhej, A. and Zahrai, S.M. (2020). "Experimental study of High Axial Damping Rubber (HADR) in new viscoelastic dampers", *Journal of Testing and Evaluation*, 48(6), 4387-4401, https://doi.org/10.1016/j.istruc.2020.12.033.

Modhej, A. and Zahrai, S.M. (2021). "Numerical study of visco-hyperelastic damper with high axial damping rubber subjected to harmonic loading", *Structures*, 29, 1550-1561, https://doi.org/10.1520/JTE20180104.

Modhej, A. and Zahrai, S.M. (2022). "Cyclic testing of a new visco-plastic damper subjected to harmonic and quasi-static loading", *Structural Engineering and Mechanics,* 81(3), 317333, https://doi.org/10.12989/sem.2022.81.3.317.

Montgomery, M. and Christopoulos, C. (2015). "Experimental validation of viscoelastic coupling dampers for enhanced dynamic performance of high-rise buildings", *Journal of Structural Engineering*, 141(5), 04014145, https://doi.org/10.1061/(ASCE)ST.1943-541X.0001092.

Nikravesh, F. and Toopchi-Nezhad, H. (2022). "Application of viscoelastic tuned mass dampers in vibration mitigation of steel joist jack arch floor structures", *Shock and Vibration*, 2022(1), 5196600, https://doi.org/10.1155/2022/5196600.

Ramakrishna, U. and Mohan, S. (2020). "Performance of low-cost viscoelastic damper for coupling adjacent structures subjected dynamic loads", *Materials Today, Proceedings*, 28, 10241029, https://doi.org/10.1016/j.matpr.2019.12.343.

Shu, Z., You, R. and Zhou, Y. (2022). "Viscoelastic materials for structural dampers, A review", *Construction and Building Materials*, 342, 127955, https://doi.org/10.1016/j.conbuildmat.2022.127955.

Smith, G., Bierman, R. and Zitek, S. (1983). "Determination of dynamic properties of elastomers over broad frequency range", *Experimental Mechanics*, 23, 158-164, https://doi.org/10.1007/BF02320404.

Suntako, R. (2017). "The rubber damper reinforced by Modified Silica Fume (MSF) as an alternative reinforcing filler in rubber industry", *Journal of Polymer Research*, 24, 17, https://doi.org/10.1007/s10965-017-1293-5.

Taleshian, H.A., Roshan, A.M. and Amiri, J.V. (2022). "Seismic pounding mitigation of asymmetric-plan buildings by using viscoelastic links", *Structures*, https://doi.org/10.1016/j.istruc.2021.11.036.

Therattil, S.J., Kuzhuppully, A.A. and Rani, J. (2008), "Compatibility studies on sulphur cured EPDM/CIIR blends", Iranian Polymer Journal, 17(6), 419-430.

Tsai, C. (1994). "Temperature effect of viscoelastic dampers during earthquakes", *Journal of Structural Engineering*, 120(2), 394-409, https://doi.org/10.1061/(ASCE)07339445(1994)120:2(394).

Vasina, M., Poschl, M. and Zadrapa, P. (2021). "Influence of rubber composition on mechanical properties", *Manufacturing Technology*, 21(2), 260-268, https://doi.org/10.21062/mft.2021.021.

Wei, W., Tan, P., Yuan, Y. and Zhu, H. (2019). "Experimental and analytical investigation of the influence of compressive load on rate-dependent high-damping rubber bearings", *Construction and Building Materials*, 200(10 March), 26-35, https://doi.org/10.1016/j.conbuildmat.2018.12.086.

Xia, L., Li, C., Zhang, X., Wang, J., Wu, H. and Guo, S. (2018). "Effect of chain length of polyisobutylene oligomers on the molecular motion modes of butyl rubber, damping property", *Polymer*, 141, 70-78, https://doi.org/10.1016/j.polymer.2018.03.009.

Xiang, Y. and Xie, H.R. (2021). "Probabilistic effectiveness of visco-elastic dampers considering earthquake excitation uncertainty and ambient temperature fluctuation", *Engineering Structures*, 226, 111379, https://doi.org/10.1016/j.engstruct.2020.111379.

Xu, Y., Xu, Z., Guo, Y., Huang, X., Dong, Y. and Li, Q. (2021). "Dynamic properties and energy dissipation study of sandwich viscoelastic damper considering temperature influence",

Buildings, 11(10), 470, https://doi.org/10.3390/buildings11100470.

Zhang, F., He, G., Xu, K., Wu, H. and Guo, S. (2015). "The damping and flame-retardant properties of poly (vinyl chloride)/chlorinated butyl rubber multilayered composites", *Journal of Applied Polymer Science*, 132(2), https://doi.org/10.1002/app.40464.

Zhang, F., He, G., Xu, K., Wu, H., Guo, S. and Zhang, C. (2014). "Damping mechanism and different modes of molecular motion through the glass transition of chlorinated butyl rubber and petroleum resin blends", *Journal of Applied Polymer Science*, 131(13), https://doi.org/10.1002/app.41259.